

Synthesis of Cu@Ag core-shell nanoparticles for characterization of thermal stability and electric resistivity

Shengyan Shang¹ · Anil Kunwar² ·
Yanfeng Wang¹ · Xiao Qi¹ ·
Haitao Ma^{1,*} · Yunpeng Wang^{1,**}

Received: date / Accepted: date

Abstract A two-step synthetic method has been utilized to prepare copper-silver (Cu@Ag) core-shell particles with thin Ag shell coated over a Cu core of initial diameter of 80 ± 5 nm. The formation of core-shell particles is characterized by transmetallation reaction on the surface of the Cu particles, where copper atoms function as the reducer for silver ions. The morphological characterization of Cu@Ag, reveals that excess supply of Ag-based reagent produces nanostructures with enhanced core-shell diameter, increased shell thickness, and agglomeration of Ag in the bulk surface; whereas limited supply of Ag species results in nanoparticles with imperfect enveloping of Cu core - making them susceptible to oxidation. Experiments with TGA and DSC, verify that thermal stability of core-shell nanoparticles is achieved for the specimen undisturbed by agglomeration and imperfect enveloping effects. Though the electrical resistivity of Cu@Ag nanoparticles increases in general with larger molar proportion of Cu, its increment rate is small for the limit [Cu]:[Ag]=4:1 and then higher beyond it. The sample with [Cu]:[Ag]=4:1, characterized by higher thermal stability, slowest oxidation speed, lower electric resistivity(

S.Y. Shang, Y. Wang, X. Qi, Y. Wang, H.T. Ma

¹School of Materials Science and Engineering, Dalian University of Technology, 116024, Dalian, China

A. Kunwar

²School of Mechanical Engineering, Dalian University of Technology, 116024, Dalian, China

*Corresponding Author

E-mail: htma@dlut.edu.cn (Haitao Ma)

Tel.: +86-0411-84707636

Fax: +86-0411-84707636 ·

**Corresponding Author

E-mail: yunpengw@dlut.edu.cn (Yunpeng Wang)

Tel.: +86-0411-84707636

Fax: +86-0411-84707636

64.24 $\mu\Omega\cdot\text{cm}$) and negligible agglomeration effect, is recommended for industrial applications.

Keywords Cu@Ag core-shell nanoparticles · electric resistivity · thermal stability · agglomeration · Oxidation

1 Introduction

Flexible electronics are widely used in radio frequency identification (RFE), solar panels, paper electronics, smart labels organic light-emitting diode (OLE), flexible circuit board (FPCB), etc. Specially, these devices need the metallic nanoparticles (NP) suspensions or pastes as conductive inks to fabricate the fine-pitch electrical line patterns. Recently, many investigations have been focused on bimetallic nanoparticles, owing to their promising characteristics. Both one-phase and two-phase alloy nanoparticles are of great interest for their improved chemical [1, 2, 3, 4], catalytic [5], optical [6, 7], biological [8] and plasmonic [9, 10] properties over their single-component counterparts [11]. The nanoparticles used within the flexible electronics devices should be characterized with excellent conductivity (least resistivity) and thermal stability. Thus, there is a significant efforts from researchers to investigate these properties of nanoparticles.

The top three metals with excellent electric conductivity are silver, copper, and gold, among which the silver is the most conductive element (6.30×10^7 Siemens meter⁻¹ at 20 °C). Moreover, its also has some other excellent properties, such as thermal conductivity, very good reflectance, anti-bacterial nature, corrosion-free capacity, etc. Despite these advantages, for the very much less abundant in the earths crust, silver is considered to be an expensive metals, which limits its wide commercial applications in the electronic packaging industry. It is well known that copper is much cheaper than silver and is the second element with high conductance after silver. At the same time, copper has got wide use as interconnecting materials in integrated circuits, owing to its high conductivity (5.988×10^7 Siemens meter⁻¹ at 20 °C) and excellent property of electromigration resistance [12]. However, due to copper nanoparticles with a very large ratio of surface area to volume, under air condition even at room temperature, it is extremely unstable to be rapidly oxidized into Cu_2O or CuO , which will significantly decrease the electrical conductivity. The lower thermal stability of Cu, is one of the main obstacles for using copper nanoparticle as conductive materials in electrical/electronic industries. Hence, there is a strong need to design a nanomaterial, that is characterized with smaller electric resistivity, high antioxidant stability and low cost. Cu@Ag core-shell nanoparticles, combining two materials, is a functional material with modified properties which can be designed to demonstrate improved physical and chemical properties, optimized cost of overall material and possible prevention of oxidation of Cu.

There are various methods to synthesis the Cu@Ag core-shell nanoparticles, such as electrochemical deposition [13], thermal evaporation [14, 15, 16],

and chemical reduction processes [17]. In present research, in order to precisely control the core size, we employ the chemical reduction method to produce the Cu nanoparticles firstly. Silver ammonia solution is utilized for preparation of Ag shell over the Cu. The solution is chosen as it advantageous for decreasing the galvanic displacement reaction speed between Cu and Ag and subsequently avoiding the possible nanoparticles agglomeration. In this research, the relative weight composition of Cu and Ag in the Cu@Ag core-shell nanoparticles was changed in order to study about the optimization of electric resistivity and thermal stability of the nanomaterials.

2 Experimental Section

2.1 Materials and Reagents

Copper sulfate pentahydrate ($\text{CuSO}_4 \cdot 5\text{H}_2\text{O}$), ammonia ($\text{NH}_3 \cdot \text{H}_2\text{O}$), pure ethanol ($\text{C}_2\text{H}_5\text{OH}$) and sodium hypophosphite monohydrate ($\text{NaH}_2\text{PO}_2 \cdot \text{H}_2\text{O}$) were supplied by Tianjin Kemiou Chemical Reagent Co., Ltd, Tianjin, China. Polyvinylpyrrolidone (PVP, $M_w = 30,000$) and silver nitrate (AgNO_3) were obtained from Sinopharm chemical reagent Co., Ltd, Shanghai, China. All these agents were used in experiment without further processing. Moreover, deionized water produced by pure water produce machine (Shanghai hitech, Master-S15). All solutions was used in all experiments for the preparation of all solutions and washing glasswares.

2.2 Cu nanoparticles synthesis

Synthesis of Cu nanoparticles was accomplished using chemical reduction method in [18]. $\text{CuSO}_4 \cdot 5\text{H}_2\text{O}$ was utilized as an initial reagent and $\text{NaH}_2\text{PO}_2 \cdot \text{H}_2\text{O}$ was selected as a reducing agent to reduce Cu^{++} ions of a solution into Cu species. PVP was used as a capping agent during the reduction reaction. As shown in Fig. 1(a), 5 g CuSO_4 and 0.02 g PVP were dissolved completely in 100 mL deionized water, a aqueous solution containing 0.02 M CuSO_4 was firstly prepared as solution A. Then, 6.36 g $\text{NaH}_2\text{PO}_2 \cdot \text{H}_2\text{O}$ was dissolved completely in 100 mL of distilled water to form the solution B. Finally, solution B was added to solution A under constant stirring of 500 r/min. With the molar ratio of N_2H_4 and CuSO_4 maintained at 3, the reaction was allowed to proceed at a temperature of 80 °C for 30 min. After the color of the mixture solution completely converted from blue to reddish brown as shown in Fig. 1, the heater power was turned off. Then, the mixture was allowed to cool naturally to room temperature for proceeding towards extraction of Cu nanoparticles. The products obtained were separated through centrifugation at 3000 rpm and then dried in the vacuum oven for 5 h at 50 °C.

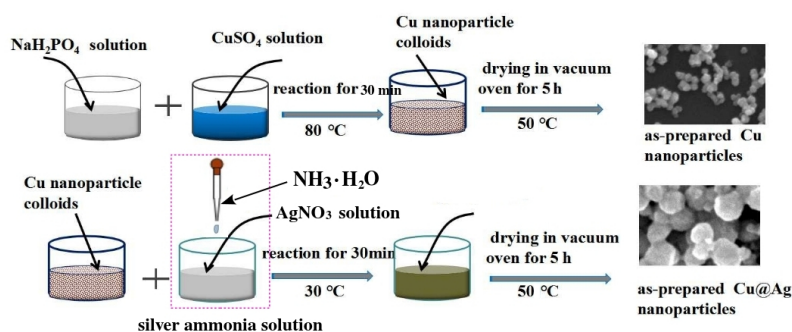


Fig. 1 A schematic diagram to illustrate the procedures for preparation of (a) Cu and (b) Cu@Ag nanoparticles via chemical reduction method.

2.3 Preparation of Cu@Ag core-shell nanoparticles

In order to prepare Cu@Ag core-shell nanoparticles, the Cu nanoparticles attained in 2.2, were washed thoroughly with ethanol to remove the excess of reducing agent, and then put into 300 mL beaker containing 50 mL distilled water (Fig. 1(b)). Inside another 150 mL beaker containing 50 ml water, AgNO_3 compound was dissolved to produce tan colored precipitate of Ag_2O . The amount of AgNO_3 put into the water was governed by the targeted molar ratio between Ag and Cu in the final core-shell particles, namely, 1, 2, 3, 4, 5 and 6. Then, dilute ammonia solution ($\text{NH}_3\cdot\text{H}_2\text{O}$) was subsequently added dropwise into the beaker containing Ag_2O precipitates. With the addition of dilute ammonia solution and maintenance of continuous stirring to the content of beaker, the precipitation would slowly start to disappear and form a clear solution. The clear solution formed from this dissolution reaction is the silver ammonia solution. The silver ammonia solution was subsequently poured into the beaker with Cu nanoparticles, and under constant stirring of 500 r/min, the reagents interact to form Cu@Ag core shell nanoparticles. The precipitated core-shell material was separated from the mixture by centrifugation and washed with ethanol + distilled water. After this, it was dried in the vacuum oven for 5 h at 50 °C. With relative molar ratio maintained between Ag and Cu during the initial preparation procedure, the resulting six types of Cu@Ag core-shell particles, had the molar ratio between core Cu and shell Ag as 1:1, 2:1, 3:1, 4:1, 5:1 and 6:1.

2.4 Characterization of Cu and Cu@Ag core-shell nanoparticles

In order to characterize the as-prepared Cu and Cu@Ag core-shell nanoparticles, they were further subjected to ultrasonication (Ultrasonic cleaner JP-040S, 10L) based dispersion in ethanol for 15 min, after the initial process of centrifugation and washing with ethanol. About 4-6 droplets of nanoparticle-ethanol suspension were poured down onto a clean silicon sheet ($4 \times 4 \times 1$

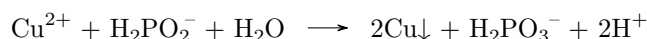
mm³) and after air drying, the sample of Cu and Cu@Ag nanoparticles were ready for SEM characterization. Field emission scanning electron microscopy (Zeiss Supra 55 FESEM) equipped with energy dispersive X-ray spectroscopy (OXFORD ISIS-3, EDS) was conducted to determine the nanoparticles size and morphology. The crystallite size and phases of the Cu nanoparticles were investigated by X-Ray diffractometer (XRD-6000). The sample was exposed to Cu K α radiation ($\lambda=1.54056 \text{ \AA}$) with the scanning speed of 2 deg/min. Similarly, the XRD patterns were obtained for Cu@Ag core-shell nanoparticles. It is to be noted that the intensity and peaks of XRD patterns are very useful in confirming about the formation of nanoparticles [19, 20, 21, 22]

The thermogravimetric analysis system (DSC822/TGA/SDTA851, Switzerland) was carried with a heating rate of 10 °C/min to investigate the thermal stability of six kinds of Cu@Ag core-shell nanoparticles, for TGA test in atmospheric condition and for DSC under nitrogen environment. Moreover, for the resistivity measurements, the testing sample was prepared by pressing the as-prepared nanopowders into a slice under an axial pressure of 20 MPa in a steel die, and cutting to a size of 10 × 10 mm. The electrical resistivity was determined from the experimental measurement with digital conductivity meter (Xamen Tianyan Sigma2008B).

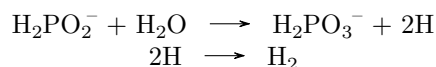
3 Results and Discussion

3.1 Formation process of as-prepared Cu@Ag core-shell nanoparticles

The synthesis of the Cu@Ag core-shell nanoparticles according to Fig. 3. Aqueous dispersion of Cu nanoparticles are prepared with the use of NaH₂PO₂·H₂O as reducing agent. Moreover, for changing the value of redox potential and tailor the reactivity of the species in a given metal-reducing-agent system needs skillful manipulations of metal complex chemistry. Firstly, at the beginning of the reaction, metal precursors were quickly reduced by H₂PO₂⁻, because of the apparently higher redox potential of H₂PO₂⁻ than Cu²⁺ according to table 1. The mechanism of Cu²⁺ reduction by H₂PO₂⁻ can be described as:



At the same time, evolution of H₂PO₂⁻ can be written as:



During the reaction process of copper sulfate solution and hypophosphite solution, the blue copper sulfate solution becomes colorless then turns green, and finally turns red wine with Cu nanoparticles formed. Fig. 2 shows the X-ray diffraction patterns for the as-prepared copper nanoparticles used in this experiment. From Fig. 2, three dominant peaks can be seen at 43.30, 50.43 and 74.13 represent (111), (200) and (220) crystal planes of metallic Cu,

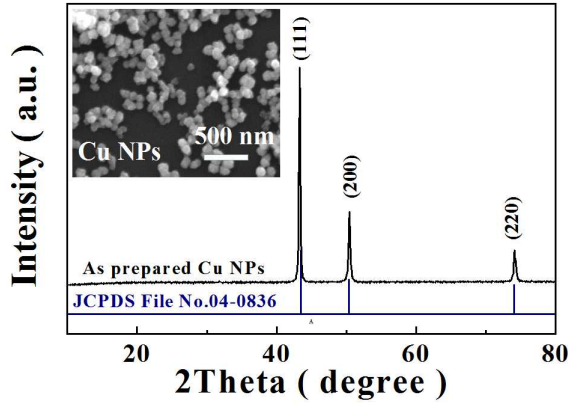


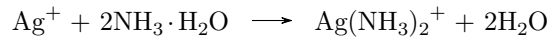
Fig. 2 XRD patterns and SEM image of Cu nanoparticles.

which confirmed that the resultant particles are pure fcc Cu. It is obvious that there is no oxide peak(s) in the XRD pattern of copper nanoparticles, which suggests the nanoparticles were protected well by the PVP without oxidation when it was exposure to the atmosphere. It will give a excellent condition for preparation of Cu@Ag core-shell nanoparticles by XRD analysis. Further more, the average crystallite size d of the samples can be estimated using the Debye-Scherrers equation:

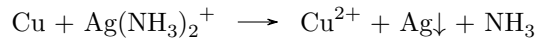
$$d = \frac{k\lambda}{\beta_{hkl}\cos\theta} \quad (1)$$

$k = 0.94$ (shape factor), λ is the Cu- K_{α} radiation of wavelength (1.5406 Å), β_{hkl} is the full width at half maximum (FWHM) in radians and θ is the scattering angle. From Scherrer's formula and full-width at half maximum (FWHM) data [23], the mean crystallite size of Cu were obtained as 80 ± 5 nm. The internal figure of Fig. 2 shows the FE-SEM images of the copper nanoparticles.

At the second step, the dilute ammonia solution have reaction with AgNO_3 forming silver ammonia solution to prevent the reduction of silver ions in solution to form free silver nanoparticles. The chemical reaction process about this as follows:



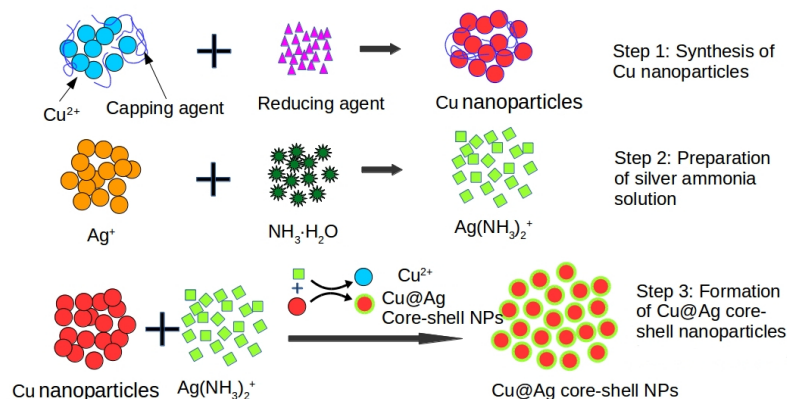
Finally, galvanic displacement reaction on the surface of Cu nanoparticles are processed between the copper atoms and the residual $[\text{Ag}(\text{NH}_3)_2]^+$ ions.



After reaction, Cu@Ag core-shell nanoparticles are obtained. It should be mentioned that the whole process is environmentally friendly without being too time or energy consuming. The reaction equations are as follows:

Table 1 Changes in the redox potential of ions for complex chemical reaction.

Redox system	E_0 (V)	Reference
$\text{Cu}^{2+} + 2e^- \rightarrow \text{Cu}^0$	+0.342	[24]
$\text{H}_2\text{PO}_2^- + \text{H}_2\text{O} \rightarrow \text{H}_2\text{PO}_3^- + 2\text{H}^+ + 2e^-$	-0.3	[25]
$\text{Ag}^+ + e^- \rightarrow \text{Ag}^0$	+0.799	[26]
$[\text{Ag}(\text{NH}_3)_2]^+ + e^- \rightarrow \text{Ag}^0$	+0.38	[26]

**Fig. 3** Schematic mechanism that explains the transmetalation method during the preparation Cu@Ag nanoparticles.

3.2 Morphology and size of Cu@Ag core-shell nanoparticles

SEM images and corresponding elemental line scanning results of obtained particles as function of the $[\text{Cu}]/[\text{Ag}]$ are shown in Fig. 4. In the figure, for line scanning results, cyan color corresponds to Ag element and red color represent Cu element in the core-shell nanoparticles. From the results of elemental mapping line scans in Fig. 4(a1)-(f1), it can be verified that the surface of core Cu were coated either completely or partially with Ag shells. When the molar ratio of $[\text{Cu}]/[\text{Ag}]$ is 1 in Fig. 4 (a), the results of EDS composition profiles along the yellow line in inner image Fig. 4 (a1), can be utilized to conclude that the nanoparticle's outer surface is nearly all Ag, which also can be speculated from Fig. 6. After galvanic displacement, the Ag content outside of the nanoparticle is increased with the Ag content at the nanoparticle surface. Therefore, excess of Ag contributed to the agglomeration between as prepared Cu@Ag core-shell nanoparticles. With the molar ratio of $[\text{Cu}]/[\text{Ag}]$ increasing, the Cu@Ag core-shell nanoparticles are less agglomerated and this corresponds to the limit of supply of Ag. The agglomeration effect is pronounced for Cu:Ag of 1:1, 1:2 and 1:3. For the molar ratio of $[\text{Cu}]/[\text{Ag}]$ is 4 in Fig. 4(d1), the surface of Cu is uniformly coated with Ag. For the nanoparticle attained with $[\text{Cu}]/[\text{Ag}]$ molar ratio at 5, Cu and Ag staggered appeared, which means Ag partially appear on the surface of Cu nanoparticles. Moreover, as the $[\text{Cu}]/[\text{Ag}]$ molar

ratio approaches 6, the elemental line scanning results shows a large junk of Cu core (red colored zone) not covered by Ag, thus rendering it susceptible to oxidation.

It can be concluded from above that the $[\text{Cu}]/[\text{Ag}]$ molar ratio strongly influence the structure and the extent of Ag covering the surface of Cu nanoparticles. The EDS results indicate that the optimized Cu@Ag core-shell nanostructures can be formed when the initial $[\text{Cu}]/[\text{Ag}]$ molar ratio is 4:1, as with this ratio both the extremely opposite features - (i) agglomeration of excess Ag, and (ii) risk of oxidation of uncovered Cu due to low supply of Ag, can be prevented.

Fig. 5 shows the change in average diameters of core-shell nanoparticles when the relative molar proportion of Cu and Ag in the initial reagents is varied. As the molar ratio $[\text{Cu}]/[\text{Ag}]$ increases, the mean diameter of the Cu@Ag core-shell particles reduces. For an example, at $[\text{Cu}]:[\text{Ag}] = 1:1$, when Ag is relatively excess, the diameter of the overall structure is 213 ± 17 nm. When the content of Ag is reduced, that is at $[\text{Cu}]:[\text{Ag}] = 6:1$, the nanoparticles have a diameter of 102 ± 5 nm. Considering the size of initial Cu nanoparticles as 80 ± 5 nm, it can be inferred that greater supply of Ag in the initial reagent solution, can enhance the shell thickness. In this present study, owing to the limitations in tracking the accurate interface between core and shell materials, the numerical values of Ag shell thickness could not be outlined experimentally. However, this work has been successful in quantifying the overall Cu@Ag core-shell thickness in relation to the initial concentrations of constituting elements; and thus subjectively predicting the Ag shell thickness. Park et al [27], have utilized FIB-SEM to locate the interface of silver-coated copper powders, and find out the measured dimensions of silver coating. A similar approach could be considered as a possible future work to resolve the interface between Cu core and Ag shell of our present study. The experiments with variation in core diameter, as outlined in [28], can also be conducted in future. The Cu core diameter's size can also potentially influence thermal stability and electrical resistivity of the resulting core-shell nanoparticles.

3.3 Thermal stability of synthesized Cu@Ag core-shell nanoparticles

To investigate the stability of the as-prepared Cu@Ag core-shell nanoparticles, XRD results of the Cu@Ag core-shell nanoparticles synthesized with different $[\text{Cu}]/[\text{Ag}]$ molar ratios after 3 month, are presented in Fig. 6. Considering the two main peaks, the intensities of Ag (111) peaks seem to decrease gradually and vice versa for those of Cu (111) with increasing Cu:Ag atomic ratios. However, for Cu@Ag core-shell nanoparticles with $[\text{Cu}]/[\text{Ag}]$ molar ratio 4, even after 3 months in ambient air, there was no obvious peaks correspond to oxides appeared in the spectra of the Cu@Ag core-shell nanoparticles, which shows the excellent air-stability of sample of $[\text{Cu}]/[\text{Ag}]$ molar ratio at 4.

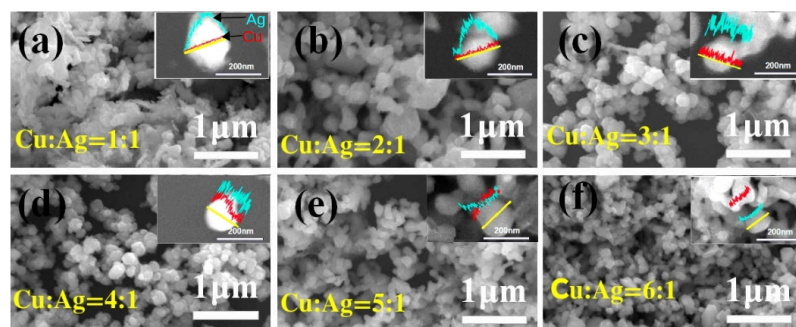


Fig. 4 The SEM images and EDS composition profiles along the yellow line of Cu@Ag nanoparticles synthesized at different molar ratio of [Cu]/[Ag], are shown in (a)-(f). The cyan and red colored line scans respectively represent Ag and Cu elements in the core-shell nanostructures.

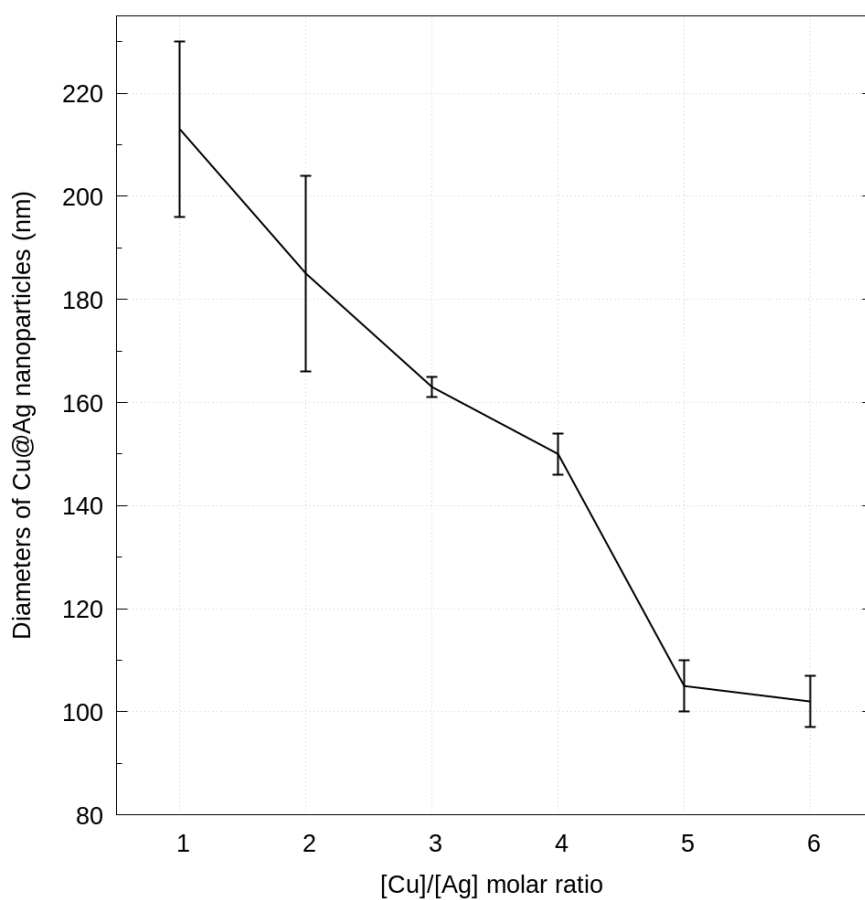


Fig. 5 The mean or average diameter of the core-shell Cu@Ag nanoparticles decreases with the reduction in relative molar concentration of Ag material.

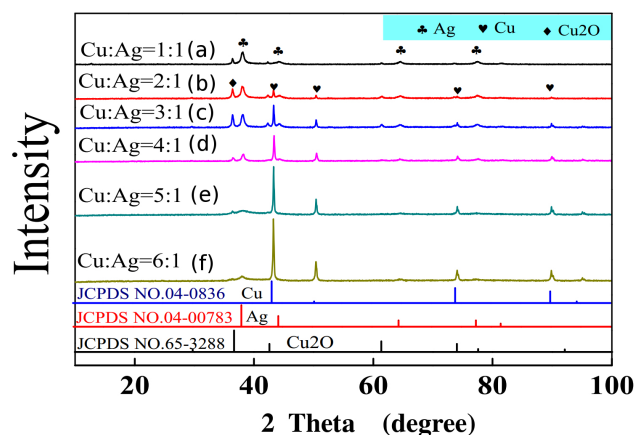


Fig. 6 The XRD spectra of Cu@Ag core-shell nanoparticles for 3 months with different [Cu]/[Ag] molar ratio.

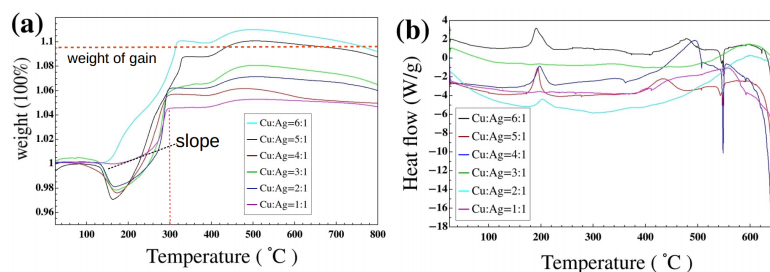


Fig. 7 TGA curve (a) and DSC (b) of the Cu@Ag core-shell nanoparticles with a heating rate of 10 °C/min.

The TGA plot of the Cu@Ag core-shell nanoparticles are shown in Fig. 7(a). More or less, there is a slight decrease on the TGA curve below 200 °C, which comes from the loss of the absorbed water and decomposition of some capping agent on the surface, corresponding to the endothermic peak at about 200 °C in the DSC thermograph in Fig. 7(b). After TGA curve slight decrease on the TGA curve below 200 °C, then the plot keeps rising before 300 °C, which shows the oxidation behavior of the Cu@Ag core-shell nanoparticles. There is no weight loss above 300 °C as all the products have been converted to oxides completely [29]. For the [Cu]/[Ag] molar ratio at 1, 2 and 3, there exists a smaller slope for slow oxidization and bigger slope for quick oxidization on the TGA plot, indicating that slow oxidization is due to the oxidation of Ag in context of the [Cu]/[Ag] molar ratio at 6. At the same time, the rapid oxidation at such lower molar fraction of Ag (e.g. [Cu]/[Ag] molar ratio at 6) is attributed to the Cu that are not totally covered by Ag and are exposed to atmospheric oxygen. Over all, the sample with [Cu]/[Ag] molar ratio at 4 has the minimal weight gain among all the experimental Cu@Ag nanoparticles.

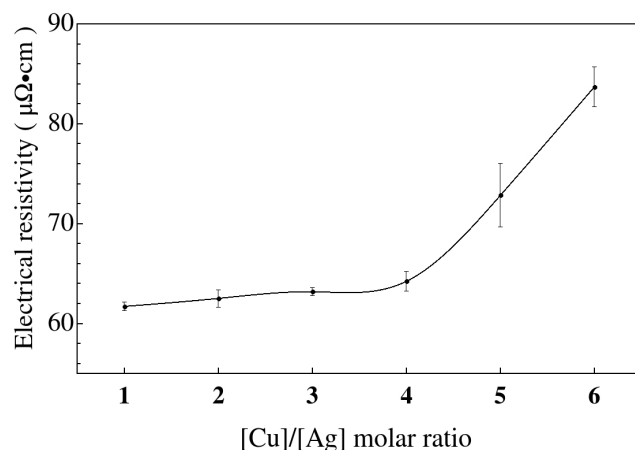


Fig. 8 The measured values of electrical-resistivity for thin sheet made by pressing Cu@Ag nanoparticles.

3.4 Electrical resistivity of as-prepared Cu@Ag core-shell nanoparticles

The results for electrical resistivity of the sheet made from pressing Cu@Ag core-shell nanoparticles, are presented for several composition proportions of Cu and Ag in Fig. 8. The results for the resistivity values are in the same order of the resistivity values for Ag nanoparticles presented in [30] and Cu-Ag nanoparticles reported in [13]. As shown in Fig. 8, the electrical resistivity increases in general with the increased molar proportion of Cu in the core-shell particles. However, it is interesting to note that the slope of resistivity curve is very low up to the molar composition $[Cu]:[Ag] = 4:1$. When the molar composition of Cu is increased beyond this limit i.e. when $[Cu]:[Ag] = 5$ and 6 , the resistivity values shoot up very high. At $[Cu]/[Ag]=1:1$ and $[Cu]/[Ag]=4:1$, average values of electric resistivity (ρ) are $60 \mu\Omega\cdot\text{cm}$ and $64.2 \mu\Omega\cdot\text{cm}$ respectively whereas the average magnitude of resistivity rises to $72.9 \mu\Omega\cdot\text{cm}$ at $[Cu]/[Ag]=5:1$ and to $83.7 \mu\Omega\cdot\text{cm}$ at $[Cu]/[Ag]=6:1$.

Among the samples containing lower proportion of Ag ($[Cu]/[Ag]=6:1$, $5:1$ and $4:1$; the sample $[Cu]/[Ag]=4:1$, is characterized with the smallest magnitude of electrical resistivity and this value is not so high as compared to $[Cu]/[Ag]=1:1$. Thus, optimization of materials costs and electrical conductivity properties, the sample $[Cu]/[Ag]=4:1$ can be selected appropriate for industrial applications.

4 Conclusions

In this research, air-stable Cu@Ag core-shell nanoparticles were synthesized by two-step synthetic method, and based upon the molar proportion of Cu and Ag in the core-shell nanostructures, they have been characterized for morphology, thermal stability and electrical resistivity properties. The following conclusions can be drawn from the study:

1. The molar composition of Cu and Ag during the procedure of nanoparticles synthesis greatly influences the morphology of the resultant core-shell nanoparticles. At excess supply of Ag reagent (e.g. [Cu]:[Ag] = 1:1), agglomeration of bulk Ag interferes with the formation of individual core-shell nanostructure. At limited supply of Ag (e.g. [Cu]:[Ag] = 6:1), most of the Cu cores are not completely enveloped by Ag shell, thus rendering the Cu susceptible to thermal oxidation. An optimized molar composition (intermediate supply of Ag), needs to be employed to solve the oppositely faced agglomeration and oxidation phenomena.
2. The Cu@Ag core-shell diameter increases with an increase in the initial molar proportion of Ag reagent.
3. From XRD and TGA results, considering the samples held for 3 months at room temperature and subjected to same magnitude of heating speed, the Cu@Ag nanoparticles with [Cu]/[Ag] molar ratio at 4:1, were observed with the slowest oxidation rate and thus are considered the one with the highest thermal stability.
4. The electrical resistivity of Cu@Ag nanoparticles, in general, has been observed to increase with the increment in the content of Cu. The increment rate of resistivity is quite small upto the sample [Cu]:[Ag] = 4:1, and for samples with Cu content higher than this limit, the increment rate is quite larger. For equal molar fraction of Cu and Ag in the nanostructures ([Cu]:[Ag] = 1:1), the mean value of measured electrical resistivity Cu@Ag core-shell nanoparticles is $61.74 \mu\Omega\cdot\text{cm}$. This value is just $64.24 \mu\Omega\cdot\text{cm}$ for sample [Cu]:[Ag] = 4:1, whereas it is around $83.7 \mu\Omega\cdot\text{cm}$ for test specimen [Cu]:[Ag] = 6:1.
5. In practical applications requiring enhanced electrical conductivity properties, higher thermal stability, reduced agglomeration effects, lowered material cost; the test specimen [Cu]:[Ag] = 4:1, can be selected as the sample characterized with optimum properties.

Acknowledgement

This work was supported by the National Natural Science Foundation of China (Grant Nos: 51571049), "Research Fund for International Young Scientists" of National Natural Science Foundation of China (Grant Number: 51750110504) and China Postdoctoral Science Foundation (Grant Number: 2017M611215).

References

1. R. Béjaud, J. Durinck, and S. Brochard. Twin-interface interactions in nanostructured Cu/Ag: Molecular dynamics study. *Acta Mater.*, 144:314–324, 2018.
2. Xue Liu, Jing Du, Yang Shao, Shao Fan Zhao, and Ke Fu Yao. One-pot preparation of nanoporous Ag-Cu@Ag core-shell alloy with enhanced oxidative stability and robust antibacterial activity. *Sci. Rep.*, 7(1):1–10, 2017.
3. Yasir Ali, Vijay Kumar, R. G. Sonkawade, M. D. Shirsat, and A. S. Dhaliwal. Two-step electrochemical synthesis of Au nanoparticles decorated polyaniline nanofiber. *Vacuum*, 93:79–83, 2013.
4. P. Konarski, I. Iwanejko, and M. Ćwil. Core-shell morphology of welding fume micro- and nanoparticles. *User Model. User-adapt. Interact.*, 70(2-3):385–389, 2003.
5. Jeremy Cure, Arnaud Glaria, Vincent Colliere, Pier Francesco Fazzini, Adnen Mlayah, Bruno Chaudret, and Pierre Fau. Remarkable Decrease in the Oxidation Rate of Cu Nanocrystals Controlled by Alkylamine Ligands. *J. Phys. Chem. C*, 121(9):5253–5260, 2017.
6. Dongxing Wang, Da Li, Javid Muhammad, Yuanliang Zhou, Ziming Wang, Sansan Lu, Xinglong Dong, and Zhidong Zhang. *<i>In situ</i>* synthesis and electronic transport of the carbon-coated Ag@C/MWCNT nanocomposite. *RSC Adv.*, 8(14):7450–7456, 2018.
7. J. Gröttrup, V. Postica, D. Smazna, M. Hoppe, V. Kaidas, Y. K. Mishra, O. Lupan, and R. Adelung. UV detection properties of hybrid ZnO tetrapod 3-D networks. *Vacuum*, 146:492–500, 2017.
8. J. Tashkhourian and S. F. Nami-Ana. A sensitive electrochemical sensor for determination of gallic acid based on SiO₂nanoparticle modified carbon paste electrode. *Mater. Sci. Eng. C*, 52:103–110, 2015.
9. Jingyi Zhao, Yuqing Cheng, Hongming Shen, Yuen Yung Hui, Te Wen, Huan-Cheng Chang, Qihuang Gong, and Guowei Lu. Light Emission from Plasmonic Nanostructures Enhanced with Fluorescent Nanodiamonds. *Sci. Rep.*, 8(1):3605, dec 2018.
10. Atrayee Hazra, Syed Minhaz Hossain, Ashit Kumar Pramanick, and Mallar Ray. Gold-silver nanostructures: Plasmon-plasmon interaction. *Vacuum*, 146:437–443, 2017.
11. G. Radnóczy, E. Bokányi, Z. Erdélyi, and F. Misják. Size dependent spinodal decomposition in Cu-Ag nanoparticles. *Acta Mater.*, 123:82–89, 2017.
12. Sushrut Bhanushali, Prakash Ghosh, Anuradda Ganesh, and Wenlong Cheng. 1D Copper Nanostructures: Progress, Challenges and Opportunities. *Small*, 11(11):1232–1252, 2015.
13. Yu Hsien Peng, Chih Hao Yang, Kuan Ting Chen, Srinivasa R. Popuri, Ching Hwa Lee, and Bo Shin Tang. Study on synthesis of ultrafine Cu-Ag core-shell powders with high electrical conductivity. *Appl. Surf. Sci.*, 263:38–44, 2012.
14. M. Cazayous, C. Langlois, T. Oikawa, C. Ricolleau, and A. Sacuto. Cu-Ag core-shell nanoparticles: A direct correlation between micro-Raman and electron microscopy. *Phys. Rev. B - Condens. Matter Mater. Phys.*, 73(11):1–4, 2006.
15. Chi-Hang Tsai, Shih-Yun Chen, Jenn-Ming Song, In-Gann Chen, and Hsin-Yi Lee. Thermal stability of Cu@Ag core-shell nanoparticles. *Corros. Sci.*, 74:123–129, 2013.
16. Chang Kyu Kim, Gyoung Ja Lee, Min Ku Lee, and Chang Kyu Rhee. A novel method to prepare Cu@Ag core-shell nanoparticles for printed flexible electronics. *Powder Technol.*, 263:1–6, 2014.
17. Jiří Sopoušek, Jiří Pinkas, Pavel Brož, Jíří Buršík, Vít Vykoukal, David Škoda, Aleš Stýskalík, Ondřej Zobač, Jan Vešál, Aleš Hrdlička, and Jan Šimbera. Ag-Cu colloid synthesis: Bimetallic nanoparticle characterisation and thermal treatment. *J. Nanomater.*, 2014, 2014.
18. Wei Li, Yansong Wang, Mengmeng Wang, Wenjiang Li, Junjun Tan, Chen You, and Minfang Chen. Synthesis of stable Cu core Ag shell & Ag particles for direct writing flexible paper-based electronics. *RSC Adv.*, 6(67):62236–62243, 2016.
19. Szu Han Wu and Dong Hwang Chen. Synthesis and characterization of nickel nanoparticles by hydrazine reduction in ethylene glycol. *J. Colloid Interface Sci.*, 259(2):282–286, 2003.

20. Yuanzhi Chen, Dong-Liang Peng, Dongxing Lin, and Xiaohua Luo. Preparation and magnetic properties of nickel nanoparticles via the thermal decomposition of nickel organometallic precursor in alkylamines. *Nanotechnology*, 18(50):505703, 2007.
21. Zhi Gang Wu, M. Munoz, and O. Montero. The synthesis of nickel nanoparticles by hydrazine reduction. *Adv. Powder Technol.*, 21(2):165–168, 2010.
22. C Thenmozhi, V Manivannan, E Kumar, and S VeeraRethinaMurugan. Synthesis and characterization of SnO₂ nanoparticles by microwave assisted solution method. *Int. Res. J. Eng. Technol.*, 02:2634–2640, 2015.
23. Hafsa Siddiqui, M. S. Qureshi, and Fozia Z. Haque. Effect of copper precursor salts: Facile and sustainable synthesis of controlled shaped copper oxide nanoparticles. *Optik (Stuttg.)*, 127(11):4726–4730, 2016.
24. Rong He, You-Cheng Wang, Xiaoyong Wang, Zhantong Wang, Gang Liu, Wei Zhou, Longping Wen, Qunxiang Li, Xiaoping Wang, Xiaoyuan Chen, Jie Zeng, and J. G. Hou. Facile synthesis of pentacle goldcopper alloy nanocrystals and their plasmonic and catalytic properties. *Nat. Commun.*, 5:1–10, 2014.
25. Jin Wen. *Preparation of surface modification copper nanoparticles and their tribological performances.pdf*. Phd, Southeast University, 2011.
26. Dan V. Goia and Egon Matijević. Preparation of monodispersed metal particles. *New J. Chem.*, 22(11):1203–1215, 1998.
27. Yu Seon Park, Chang Yong An, Padmanathan Karthick Kannan, Nary Seo, Kai Zhuo, Tae Kyong Yoo, and Chan Hwa Chung. Fabrication of dendritic silver-coated copper powders by galvanic displacement reaction and their thermal stability against oxidation. *Appl. Surf. Sci.*, 389:865–873, 2016.
28. Jit Sarkar and D. K. Das. Study of the effect of varying core diameter, shell thickness and strain velocity on the tensile properties of single crystals of CuAg core-shell nanowire using molecular dynamics simulations. *J. Nanoparticle Res.*, 20(1), 2018.
29. Jian Quan Qi, Hu Yong Tian, Long Tu Li, and Helen Lai Wah Chan. Fabrication of CuO nanoparticle interlinked microspheres by solution method. *Nanoscale Res. Lett.*, 2(2):107–111, 2007.
30. Ian E. Stewart, Myung Jun Kim, and Benjamin J. Wiley. Effect of morphology on the electrical resistivity of silver nanostructure films. *ACS Appl. Mater. Interfaces*, 9(2):1870–1879, 2017.